Published in final edited form as:
Inhal Toxicol. 2007 April ; 19(4): 333–342. doi:10.1080/08958370601144241.

Particle Size Distribution and Inhalation Dose of Shower Water Under Selected Operating Conditions

Yue Zhou, **Janet M. Benson**, **Clinton Irvin**, **Hammad Irshad**, and **Yung-Sung Cheng**
Lovelace Respiratory Research Institute, Albuquerque, New Mexico, USA

Abstract

Showering produces respirable droplets that may serve to deposit pollutants such as trihalomethane decontamination products, heavy metals, inorganic salts, microbes, or cyanoacterial toxins within the respiratory tract. The extent and importance of this route of indoor exposure depend on the physical characteristics of the aerosol as well as the pollutant profile of the source water. The purpose of this study was to characterize shower-generated aerosols as a function of water flow rate, temperature, and bathroom location. Aerosols were generated within a shower stall containing a mannequin to simulate the presence of a human. Using hot water, the mass median diameter (MMD) of the droplets inside the shower and in the bathroom were 6.3–7.5 um and 5.2–6 μm, respectively. Size was independent of water flow rate. The particle concentration inside the shower ranged from 5 to 14 mg/m^3. Aerosols generated using cold water were smaller (2.5–3.1 μm) and concentrations were lower (0.02–0.1 mg/m^3) inside the shower stall. No aerosols were detected in the bathroom area when cold water was used. The International Commission on Radiological Protection model was used to estimate water deposition in the respiratory tract. For hot water, total deposition ranged from 11 to 14 mg, depending on water flow rate, with approximately 50% of this deposited in the extrathoracic region during assumed mouth breathing, and greater than 86% when nose breathing was assumed. Alveolar deposition was 6–10% and 0.9% assuming oral and nasal breathing, respectively. The consequences deposition of shower water droplets will depend on the nature and extent of any pollutants in the source water.

One potential source of human exposure to environmental pollutants is through chemically contaminated domestic tap water. The most obvious route of exposure to contaminants is by ingestion; however, dermal and inhalation exposure may also occur within the home. Several studies have shown that showering increases the likelihood that an organic compound will be volatilized, resulting in human exposure beyond that occurring from ingestion (Backer et al., 2000; Giardino & Hagman, 1996; Kerger et al., 2000; Moya et al., 1999; Prichard & Gesell, 1981). For example, in one study, the blood levels of trihalomethane were highest among individuals showering for 10 min, intermediate for individuals bathing for 10 min, and lowest among those who drank 1 L water from the same source over a 10-min period (Backer et al., 2000). These results support the hypothesis that showering is an important route of exposure for trihalomethanes, and possibly other volatile contaminants in tap water.

Address correspondence to Yue Zhou, 2425 Ridgecrest Dr. SE, Albuquerque, NM 87108, USA. yzhou@lrri.org.

Domestic water supplied from wells and municipal water systems may also be contaminated with heavy metals such as arsenic, chromium, and lead that have documented respiratory-tract and/or systemic toxicities following inhalation. Further, cyanobacterial toxins are being found with increasing frequency in surface waters worldwide (Falconer, 1994). Microcystins produced by cyanobacteria are hepatotoxic, are tumor promoters, and produce nasal lesions when inhaled (Benson et al., 2005, and references sited therein). Recent studies by Cohen and Ollison (2006) and Xu and Weisel (2003) demonstrated that water droplets formed in bathroom showers contain a respirable fraction, and therefore could serve as potential vectors for respiratory-tract deposition of potentially toxic contaminants of tap water.

The purpose of this study was to examine the characteristics of shower water aerosols as a function of water flow rate, temperature, and location within a model bathroom. Total and regional respiratory-tract deposition of water as wells as for selected pollutants present in the local water supply were calculated. Results will be useful in calculating the potential risk from shower water exposure, depending on the nature and concentration of contaminants in a given water supply.

EXPERIMENTAL APPROACH, MATERIALS, AND METHODS

Bathroom and Shower Stall

Sampling took place in a bathroom at the Lovelace Respiratory Research Institute (Figure 1), having dimensions of 3.75 m long × 1.85 m wide × 2.4 m high (total volume = 16.7 m^3). The ventilation of the bathroom was controlled by the building's central ventilation system. The shower stall had a total volume of 2.0 m^3 (0.92 m × 0.92 m × 2.41 m) with a 0.35-m gap between the shower wall and ceiling. A regular mannequin (1.70 m high) without heating system in the body was positioned in the shower 0.8 m away from the showerhead. The water was showered on the chest of the mannequin with an angle of approximately 30°. The sampling position was at the height of mannequin's breathing zone (1.50 m from the shower floor), inside (position A) and outside (position B) the shower stall (Figure 1).

Exposure Parameters

Three different showerheads (A, B, and C) were used in the study, producing three different flow rates. All showerheads used were within the federal requirement that limits water flow rate to 9.5 L/min (2.5 G/min). The flow rates were 5.1, 6.6, and 9.0 L/min for showerheads A, B, and C, respectively, with a pressure drop of 40–42 psi. The shower pattern was continuous without any pause. The characteristics of each showerhead are summarized in Table 1. The temperature of the hot water was controlled at 43–44°C. The water temperature measured at the mannequin was 35–37°C. For comparison, the test was also conducted with cold water at a temperature of 24–25°C under the same conditions. Table 1 shows the exposure parameters of this study.

The particle size distribution of the shower spray was very wide. However, only inhalable particles were of interest in the study. The total mass concentration of particles was determined using a DataRAM real-time particle monitor (Monitoring Instruments for the Environment, Inc., Bedford, MA). This instrument measures particles in the concentration range of 0.1 μg/m^3– 400 mg/m^3 for particles less than 10 μm in diameter. Because the DataRAM is a nephelometer-based instrument, relative humidity can confound it. In order to measure the droplets, the DataRAM was calibrated with a quartz crystal microbalance cascade impactor (model PC-2, California Measurement, Inc., Sierra Madre, CA). Results measured by DataRAM were corrected by the calibration curve. The second instrument was an Aerodynamic Particle Sizer (APS 3310; TSI, Inc., Amherst, MA), measuring particle number and mass size distributions. The particle size range by APS measurement was 1–30 μm with phantom

correction. The APS instrument completed 1 measurement every minute, so 10 replicate measurements were made during each 10-min showering period. The relative humidity (RH) was measured using a humidity/temperature datalogger (model 800014; SPER Scientific Ltd., Scottsdale, AZ) with a 6-s interval. The RH was recorded during the entire study period.

The air exchange rate, regulated by the building's air handling system, was measured using a trace gas technique (Cheng et al., 1995). A predetermined amount of sulfur hexafluoride (SF_6) in a compressed gas cylinder was released into the room to give an initial concentration of between 10 and 100 ppb. The SF_6 concentration was monitored using an AutoTrac monitor (model 101; Lagus Applied Technology, Inc., San Diego, CA) positioned at the center of the bathroom. Changes in the air exchange rate were investigated under various conditions when the bathroom doors were open or closed. Assuming that the air in the bathroom is well distributed, the air exchange rate can be obtained by fitting the SF_6 concentration versus time to an exponential decay curve over a period of 2 h.

Sampling Protocol

All instruments were switched on a few minutes before the shower was turned on. The shower was run for 10 min. The curtain of the shower stall was opened 2 min after the shower was turned off. Five minutes later, the bathroom doors were opened to increase the ventilation. The next test period began when the room temperature and RH were back to baseline values. The protocol was conducted with probes in the shower stall (position A) and bathroom (position B) for hot and cold water.

Data Analysis

Particle Distribution—A lognormal particle size distribution was assumed. The mass median diameter (MMD) and the geometric standard deviation (GSD) were calculated with a technical graphing software, SigmaPlot (SPSS, Inc., Chicago).

Generation Rate—The generation rate of shower-water particles in this study was calculated using the method of Zhou and Cheng (2000). The generation rate was assumed to be constant because the water pressure (and therefore flow rate) was monitored and remained constant during the 10-min runs. The temporal changes in the particle concentration, C_i, can be described by the following equation (Cheng et al., 1995):

$$\frac{dC_i}{dt} = G - (\lambda_v + \lambda_w)C_i \quad [1]$$

where G is the generation rate in μg/m^3/min, λ_v is the air exchange rate in the bathroom, and λ_w is the rate of particle losses due to deposition on the shower wall, floor, and body of mannequin in reciprocal minutes. This equation can be solved with the initial condition of t = 0 and C_i = 0, leading to the analytical solution for particle concentration:

$$C_i = \frac{G}{\lambda}(1 - e^{-\lambda t}) \quad [2]$$

where $\lambda = \lambda_v + \lambda_w$.

Exponential rise regressions were carried out with a commercial software, Table Curve (SPSS, Inc.), to obtain the generation rate.

Dose Calculation—Particle deposition fractions in human lungs were calculated using the computer software LUng Dose Evaluation Program (LUDEP), implementing the model of a human respiratory tract as documented in ICRP Publication 66 (ICRP, 1994). In this model, human activities are classified into four statuses: sleeping, sitting awake, light exercise, and heavy exercise. We assumed that showering was light exercise and that the showering period was 10 min. Deposition was calculated in two ways, assuming either mouth breathing or nose breathing. The dose with mixed breathing should be within those parameters. The ICRP deposition model was also used to calculate the particle deposition fractions in four regions: extrathoracic (ET), bronchial (BB), bronchiolar (bb), and alveolar (Al), for inhaled particles.

RESULTS

The SF_6 gas concentration decreased with the time as the bathroom doors were closed and opened. The air exchange rate in the bathroom was calculated as 1.17/h and 1.62/h for closed or open, respectively, which is 2 times higher than the mean indoor exchange rate of a whole house (0.53/h, U.S. EPA, 1996).

Particle size distribution did not vary over the 10-min showering time (data not shown). Particle size distributions in the shower stall during a 1-min sampling period are compared in Figure 2 and Figure 3 for hot and cold water at the three flow rates inside the shower stall (sampling position A). For comparison, particle size distributions were also measured in the bathroom but outside of the shower stall (sampling position B). Figure 4 shows the particle size distributions at a flow rate of 5.1 L/min inside and outside of the shower stall. Because particle concentration in the bathroom area during showering with cold water was close to background, no particle size distribution for these particles was obtained. The MMD was about 20–40% higher in the shower stall than in the bathroom. Detailed information related to the MMD and GSD for all tests is provided in Table 2.

Figure 5 shows the particle concentrations and the RH for cold water (Figure 5.1) and hot water for showerheads A, B, and C, corresponding to flow rates of 5.1, 6.6, and 9.0 L/min, inside (Figure 5.2) and outside (Figure 5.3) the shower stall. The hot-water particle concentration in the shower stall was somewhat variable, especially within the first 5 min of showering. The concentrations ranged from 300 $\mu g/m^3$ to 14,000 $\mu g/m^3$. The highest concentration was obtained with a higher RH, which is about 80%. For cold water, it is clear from Figure 5 that the particle concentration was lower with a low flow rate. As expected, the RH for cold water was stable and much lower compared with hot water. The particle concentration of the cold water shower (from 20 to 100 $\mu g/m^3$) was also much less than that of the hot-water shower.

Particle generation rates were obtained from concentration/time data in the first 10 min of showering, as shown in Figure 6.1 (for cold water) and Figure 6.2 (for hot water). The curves are best-fitted curves for each flow rate (showerhead) using Eq. (2). The zero time begins when the water temperature reaches 44°C for hot water showering. The generation rates (G) and λ values in Eq. (2) are provided in Table 2. Basically, generation rate increases as the flow rate increased. The ratio of G and λ represents the generated particle concentration.

The ICRP (1994) suggested a tidal volume of 1.25 L and a respiration frequency of 20 breaths/min for an adult male performing light exercise. Thus, the total air volume inhaled during a 10-min shower is 0.5 m^3. The deposition doses in different regions of the human lung are listed in Table 3 for mouth and nose breathing. No MMD and GSD for cold-water aerosols generated using a flow rate of 9.0 L/min were obtained because the aerosol particle size distribution was not lognormally distributed. Therefore, the particle deposition fraction in lung regions was calculated using a specific size ranging from 0.5 to 30 μm and their distribution fraction.

DISCUSSION

Particle Size Distribution

As shown in Figure 2, particle size distribution was only mildly affected by water flow rate for the hot water experiments. Therefore, flow rate was considered not to affect the extent of deposition of water droplets in the respiratory tract. This indicates that particles would deposit into the human respiratory system with a same deposition fraction. However, for cold water, as shown in Figure 3, the particle distribution varied significantly with flow rate. Particles had a lognormal distribution with a flow rate of 5.1 L/min, a slight deviation from lognormal distribution with the flow rate of 6.6 L/min, and totally non-lognormal distribution with the flow rate of 9.0 L/min. Particle size increased with flow rate. The concentration of large particles increased as the flow rate increased. This indicates that many droplets generated from a high-flow-rate showerhead did not have enough time to evaporate when they reached the sampling probe. Thus, the particle deposition in the respiratory tract for cold-water showering is dependent on water flow rate. The results of particle size distribution inside and outside the shower stall (Figure 4) indicates that droplets escaping from the shower stall and reaching the bathroom had more time to evaporate than those in the shower stall. Although the RH in the room was around 80%, evaporation could still take place as long as the air was not saturated. The particles from the cold water had the smallest MMD with the largest GSD. This is because room humidity is lower than that during hot water showering. The evaporation rate for the cold water droplets is higher than that for the hot water droplets.

Only one publication was found to date studied shower particle size distribution. Giardino and Hageman (1996) discussed the drop-size distribution compared with some theoretical models. The particle distribution was in the millimeter size range according to their study. Their results differed from those in this study, possibly because the showerhead was positioned horizontally and because they did not use a shower stall.

Particle Concentration

The particle concentration differences with hot and cold water may stem from a hot-water chimney effect within the stall. Micrometer-sized satellite droplets are formed with spray droplet formation from the showerhead, from splashing on the mannequin, and from splashing against the stall walls and floor. The satellite droplets evaporate within seconds at RH <90% and are carried upward in the chimney-like convective flow within the stall that is created by the hot water heating the stall air. Downward flow may occur when the cold water temperature is below room temperature, assuming that the shower curtain does not wholly prevent such flows at the top and bottom of the stall. Placed at the breathing zone, the sampler inlets may under sample fine-particle (<2.5 μm) concentrations for cold showers but more reliably sample fine particles for hot showers in the stall because fine particles are convected upward from lower levels within the stall. A relatively low fine-particle concentration (Figure 5.1) indicates stratification, with most of the particle-rich air staying below the stall's sampling point. In Figure 5.2, a relatively high fine-particle level was obtained due to an upward convective flow that brings particle-rich air past the stall's sampling inlet. A sharp drop at point B of Figure 5.2 indicates the passing bottom edge of a rising plume of particle-rich air from below in the stall after the shower was turned off. By comparison, hot-water particle concentration in the bathroom (outside of the shower stall, Figure 5.3) was much lower than that inside shower stall. The outside stall sampling was likely to miss many particles due to stratification of fine-particle-rich air at the ceiling for hot showers and at the floor for cold showers, indicating that the volume of air in the bathroom was not well mixed.

Xu and Weisel (2003) also reported that when showering at a temperature of 36–38°C, a particle size smaller than 2 μm with a peak concentration of 414 ± 258 $\mu g/m^3$ was obtained. This

concentration was much lower than our results. There are several factors that could cause the differences between the two studies. In the Xu and Weisel study, air was sampled through a 1.75-m stainless tube, resulting in sampling line losses. In addition, the study of Xu ad Weisel (2003) didn't include a mannequin, thereby causing a lower particle concentration in the shower stall.

The particle number concentration of this study was also compared with the study of Cowen and Ollison (2006). In our study, the number concentration for the particles below 2.5 μm was about one order of magnitude greater than the data of Cowen and Ollison (2006). Two reasons possibly account for this difference. The air exchange rate of their study was 6/h, which is much higher than our study. The water temperature of their study (39°C) was about 4–5 degrees lower than ours.

Inhalation Dose

The result in Table 3 shows that the total deposited dose of water increased with increasing flow rate for both cold and hot water. The deposited water dose for hot water is 50–100 times higher than that for cold water. For hot water, 64–70% of the total dose was deposited in the ET region, but still about 10% (~1.0 mg) was deposited in the Al region. Because the particle generation rate of cold-water showering was very low, the deposition dose was very low, even for the large particles generated at 9.0 L/min. Because of the large particle size of the aerosols, total deposited dose was slightly higher for nasal compared to mouth breathing, and alveolar deposition was greater with mouth breathing. Deposition in the Al region was much higher for oral than for nose breathing. From the deposited dose of water calculated in this study, the corresponding deposited doses for specific water contaminants can be also calculated when the concentrations of contaminants are known. As an example, the deposition doses of several elements in Albuquerque city water supply were calculated (Table 4), based on the local water quality report (City of Albuquerque, 2005). As expected, the calculated deposition of contaminants is greater with hot-water showering compared to when cold water was used. The inhalation dose of hot-water showering appears about two orders of magnitude higher than that of cold water for various elements. Although the deposition doses of the chemicals are quite low, the contaminants may indeed deposit in respiratory tract, primarily the upper respiratory tract, during showering.

CONCLUSIONS

The characteristics of shower water aerosols in a model bathroom have been examined as a function of water flow rate, temperature, and location in the bathroom. Particle size distribution indicates that the majority of the aerosol is deposited in the upper respiratory tract and thoracic region. The consequences of this deposition will depend on the nature and extent of contaminants in the source water. The results of this study may assist in others with indoor air pollution model development.

Acknowledgments

The authors are grateful to Dr. Will M. Ollison of the American Petroleum Institute for his review of this article and very useful comments, and V. Fisher of the Lovelace Respiratory Research Institute for technical editing. This research is supported by the NIEHS program project P01-ES10594.

REFERENCES

Backer LC, Ashley DL, Bonin MA, Cardinali FL, Kieszak SM, Wooten JV. Household exposures to drinking water disinfection by-products; Whole blood trihalomethane levels. J. Expos. Anal. Environ. Epidemiol 2000;10:321–326.

Benson JM, Hutt JA, Rein K, Boggs SE, Barr EB, Walsh P, Fleming LE. The toxicity of microcystin LR in mice following 7 days of inhalation exposure. Toxicon 2005;45:691–698. [PubMed: 15804518]

Cheng YS, Bechtold WE, Yu CC, Hung IF. Incense smoke: characterization and dynamics in indoor environments. Aerosol. Sci. Technol 1995;23:271–281.

City of Albuquerque. Water quality report. 2005. Available from http://www.cabq.gov/waterquality

Cowen KA, Ollison WM. Continuous monitoring of particle emissions during showering. J. Air Waste Manage. Assoc 2000;56:1662–1668.

Falconer IR, Burch MD, Steffensen AD, Choice M, Coverdale BR. Toxicity of the blue-green algae (cyanobacterium) *Microcystis aeruginosa* in drinking water to growing pigs, as an animal model for human injury and risk assessment. Environ. Toxicol. Water Qual 1994;9:131–139.

Giardino NJ, Hageman JP. Pilot study of radon volatilization from showers with implications for dose. Environ. Sci. Technol 1996;30:1242–1244.

International Commission on Radiological Protection. Ann. ICRP Publication. Vol. 66. Oxford: Pergamon Press; 1994. Human respiratory tract model for radiological protection.

Kerger BD, Schmidt CE, Paustenbach DJ. Assessment of airborne exposure to trihalomethanes from tap water in residential showers and baths. Risk Anal 2000;20:637–651. [PubMed: 11110211]

Moya J, Howard-Reed C, Corsi RL. Volatilization of chemicals from tap water to indoor air from contaminated water used for showering. Environ. Sci. Technol 1999;33:2321–2327.

Prichard HM, Gesell TF. An estimation of population exposures due to radon in public water supplies in the area of Houston, Texas. Health Phys 1981;41:599–606. [PubMed: 7309518]

U.S. Environmental Protection Agency. air quality criteria for particulate matter. Vol. Volume I of III. Washington, DC: U.S. EPA; 1996 Apr. p. 7-58.EPA/600/P-95/001aF

Xu X, Weisel CP. Inhalation exposure to haloacetic acids and haloketones during showering. Environ. Sci. Technol 2003;37:569–576. [PubMed: 12630474]

Zhou Y, Cheng YS. Characterization of emissions from kerosene heaters in an unvented tent. Aerosol Sci. Technol 2000;33:510–524.

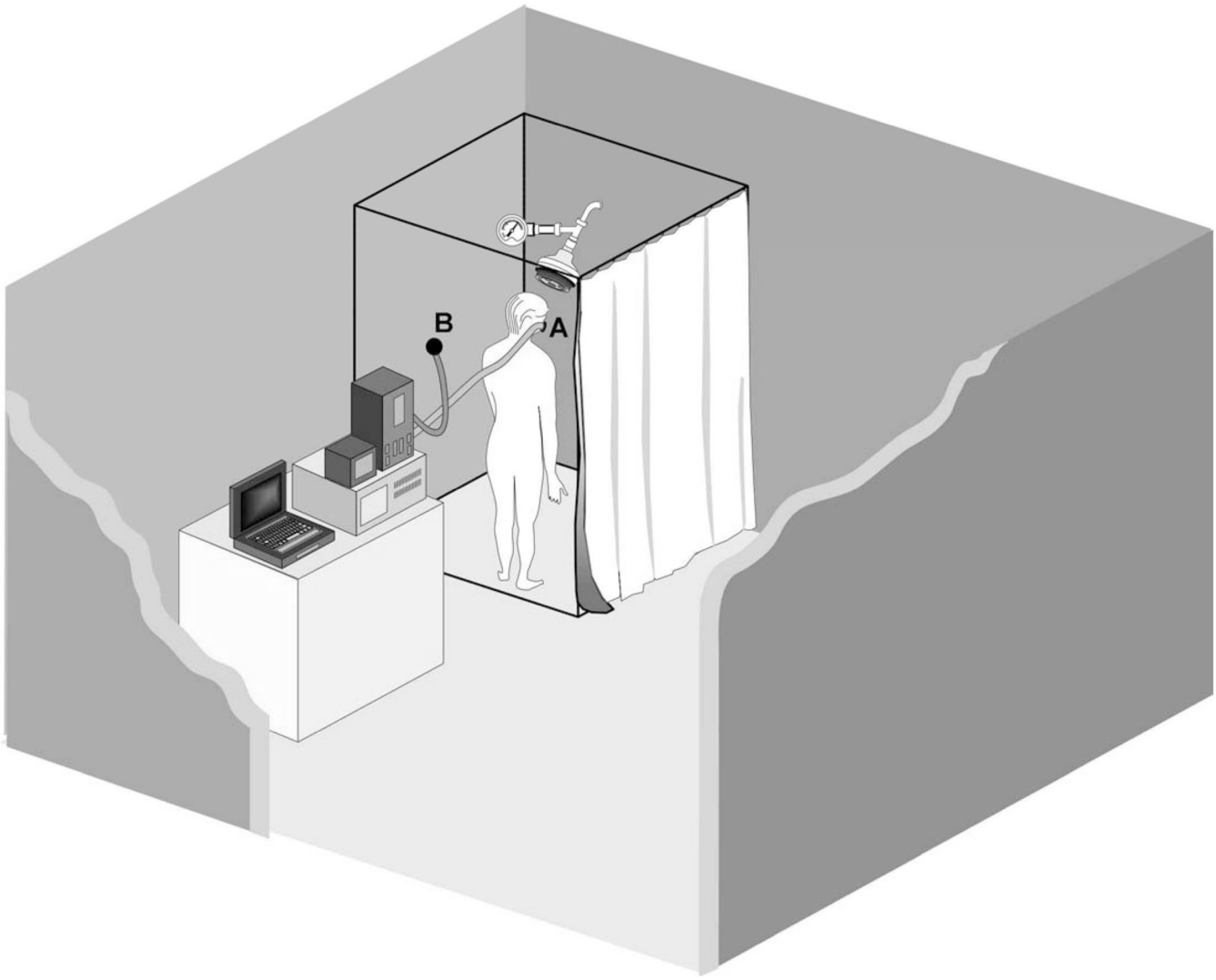

FIG. 1.
Schematic of the experimental setup, including the sampling positions A and B.

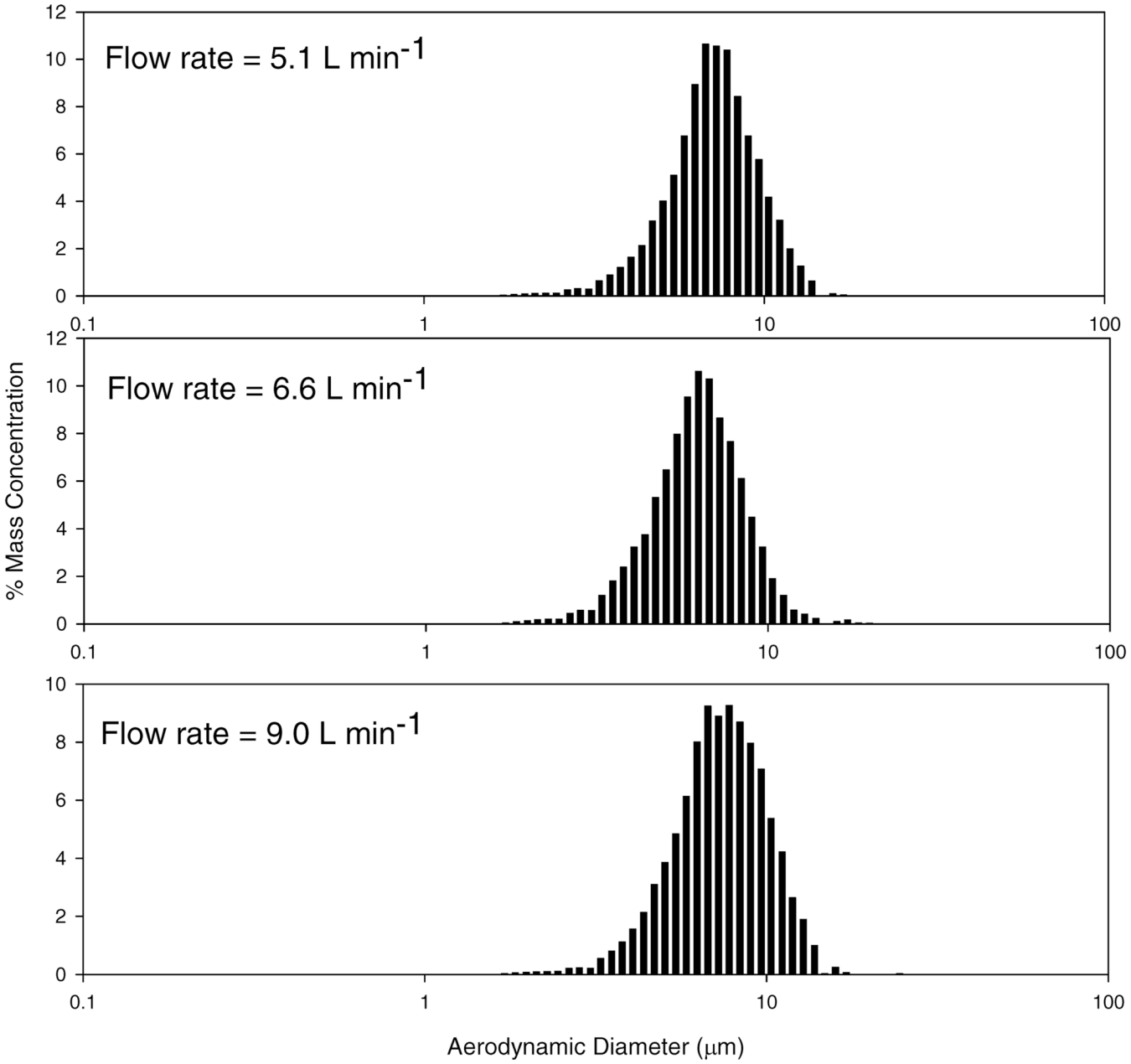

FIG. 2.
Particle distributions with hot water at various flow rates.

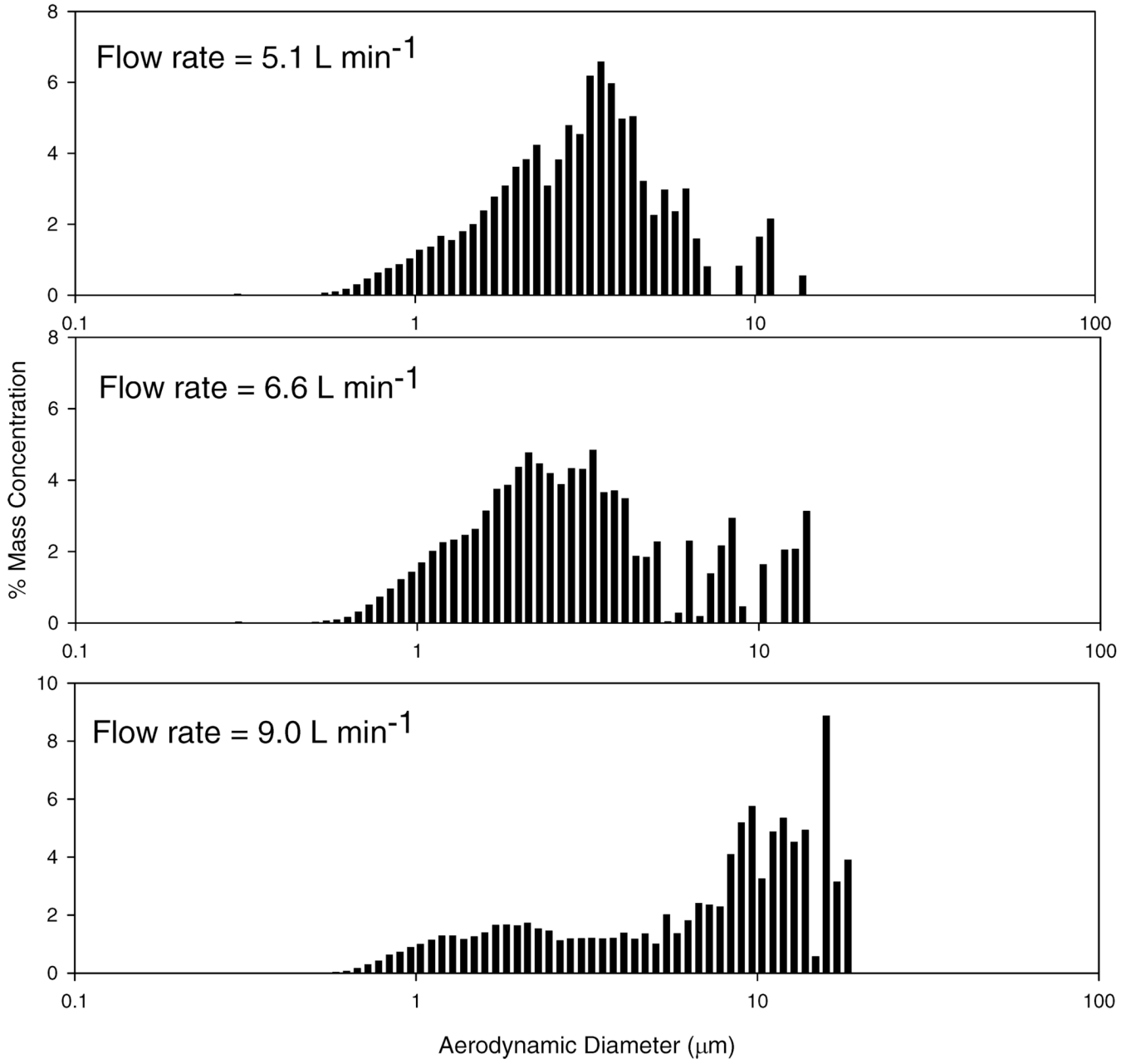

FIG. 3.
Particle distributions with cold water at various flow rates.

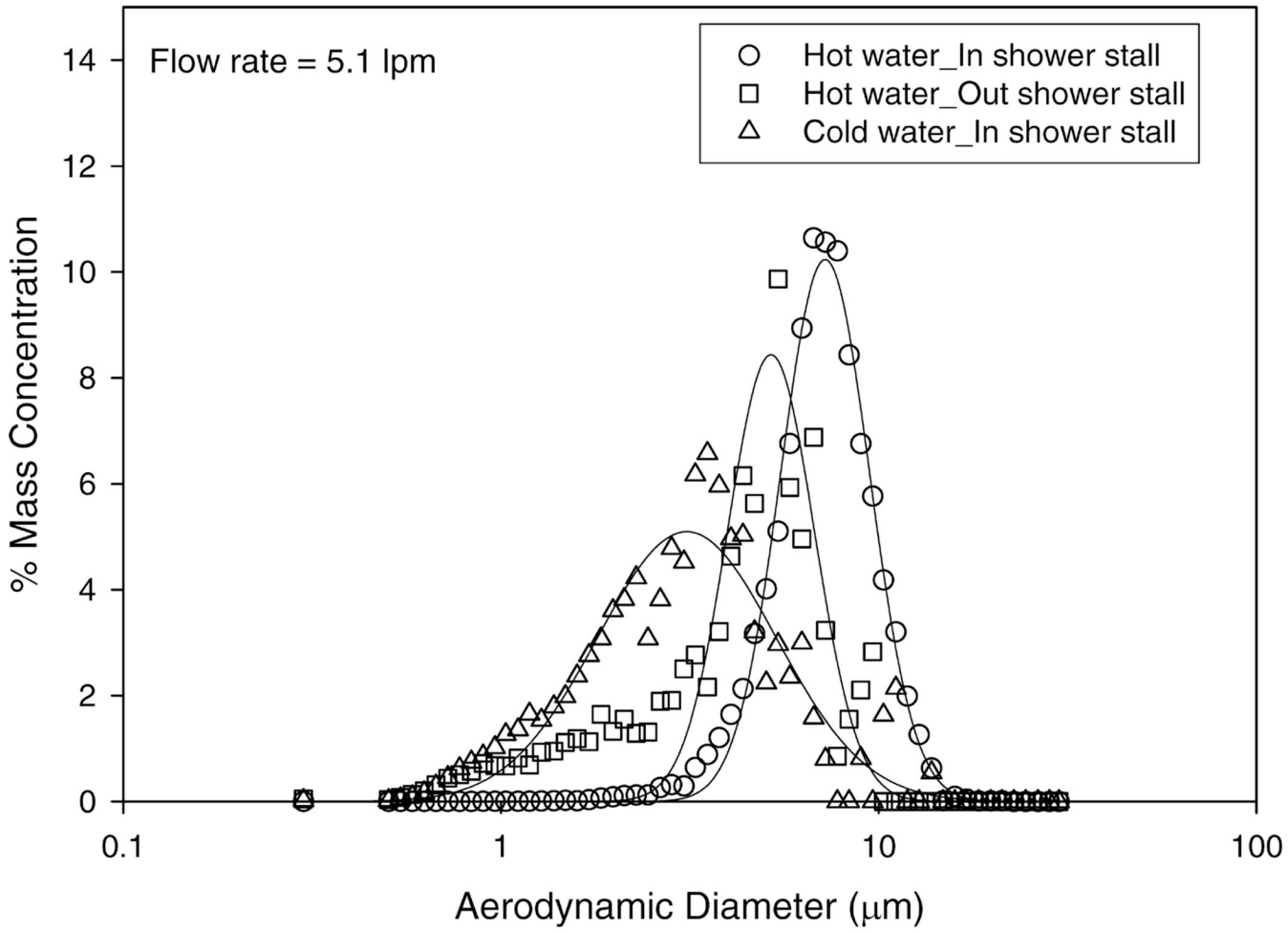

FIG. 4.
Particle distribution comparison with different sampling positions and water temperatures at a flow rate of 5.1/L min^{-1}.

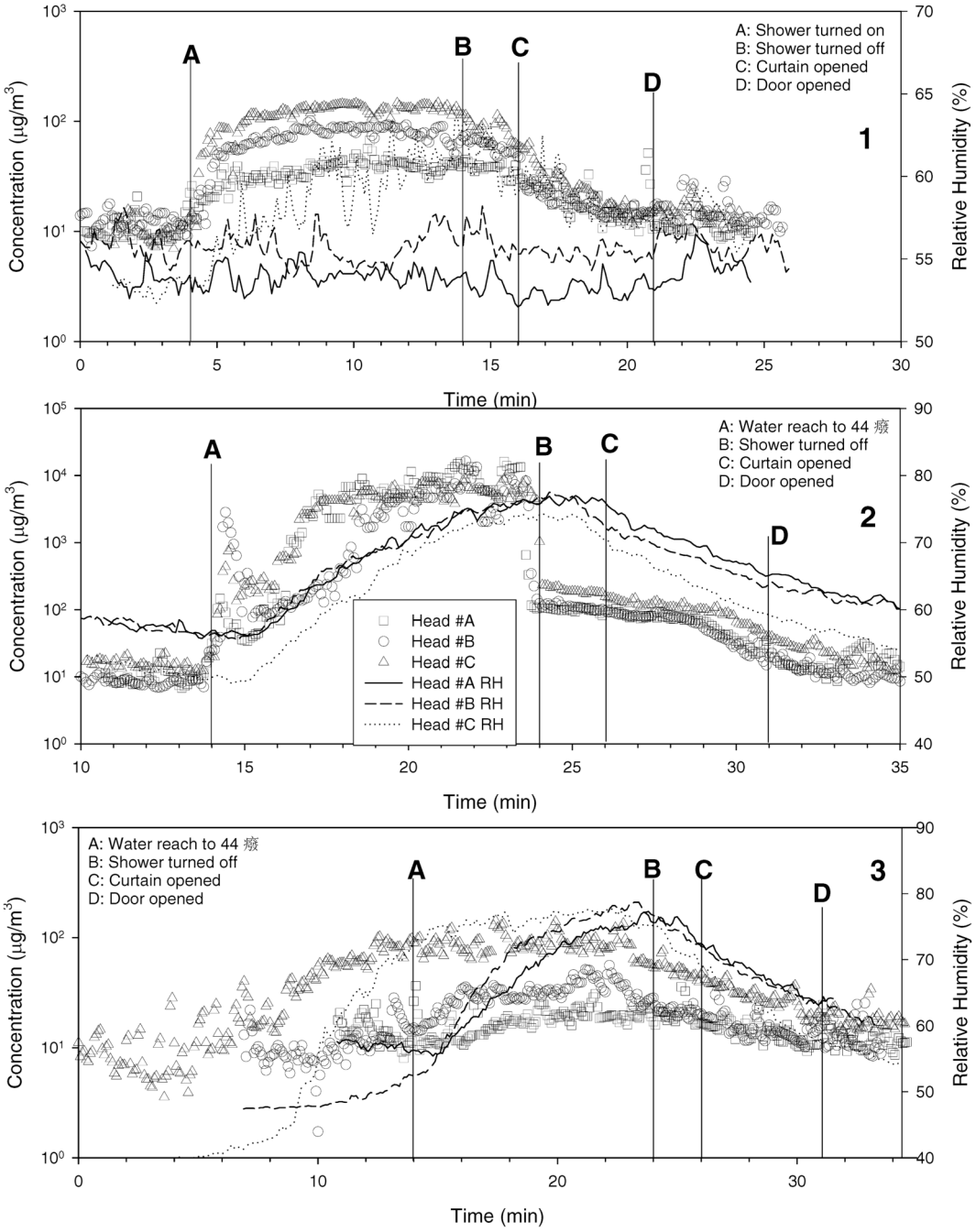

FIG. 5.

Particle concentration profiles for the cold water inside the shower stall (1), the hot water inside the shower stall (2), and the hot water outside the shower stall (3).

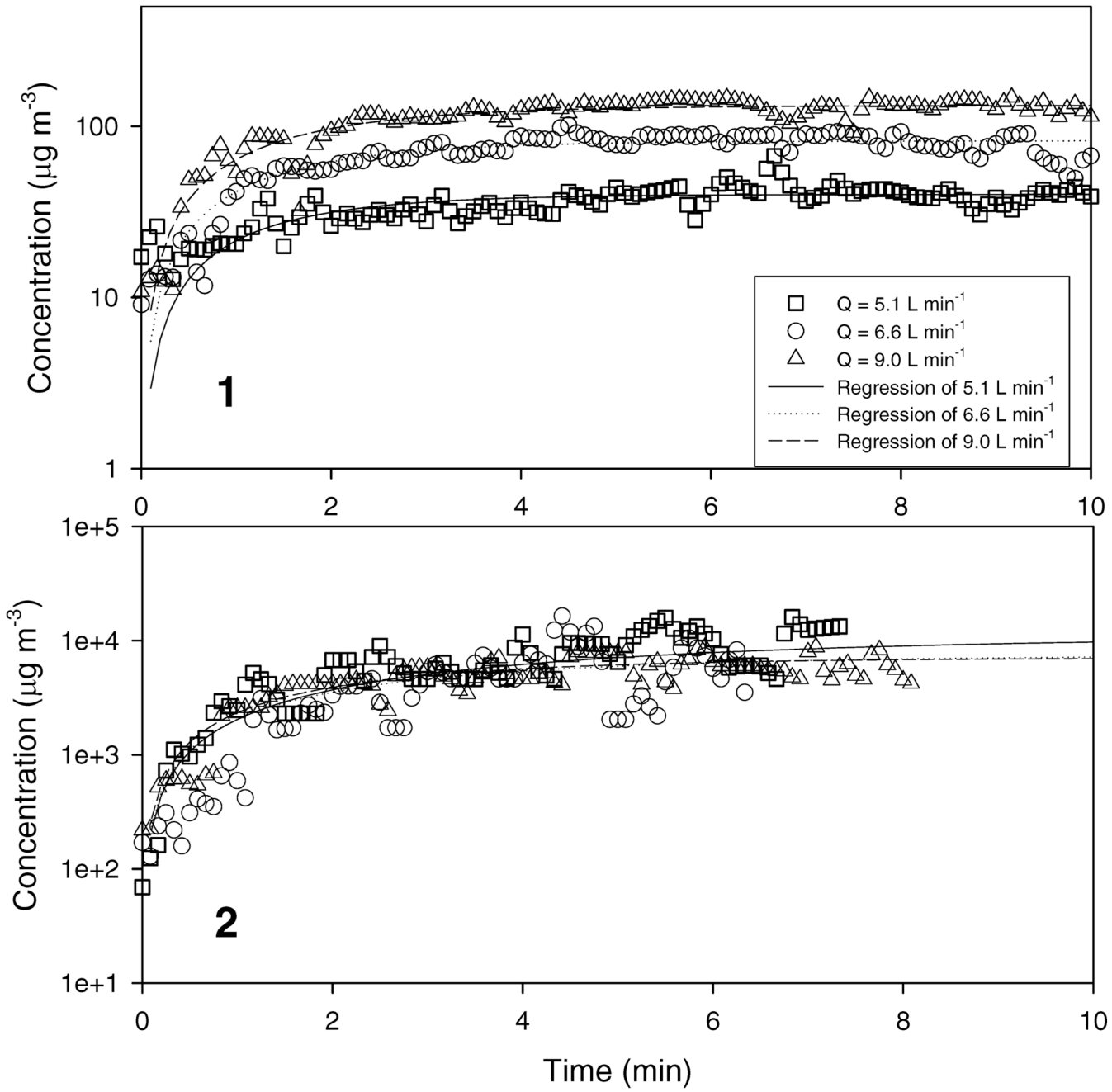

FIG. 6.
Generation rate regressions for the cold-water shower (1) and the hot-water shower (2) at various flow rates.

TABLE 1

Exposure parameters of the study

Shower head	Jet size (mm)	Number of jets	Spray area (cm^2)	Pressure (PSI)	Flow rate (L/min)	Hot water temperature (°C)		Cold water temperature (°C)	
						Showerhead	Mannequin	Showerhead	Mannequin
A	1.15	54	23.7	40	5.5				
B	1.20	10[a]	3.1	42	6.1	43–44	35–37	24–25	24–25
C	1.05	24[b]	19.6	40	9.0				

[a]The water dispersing plate contains eight narrow slits located around the jets.

[b]The water dispersing plate contains six holes distributed on a 50-mm circle, and each hole contains four jets.

TABLE 2

Particle characterization and the generation rate at various conditions

	Flow rate (L/min)	CMD[a] (μm)	MMD[b] (μm)	GSD[c] for CMD	GSD for MMD	G[d] (μg/m^3 min)	λ[e] (/min)	G/λ (μg /m^3)
Cold water	5.1	0.96	3.10	1.59	1.73	30.79	0.77	40.0
	6.6	0.87	2.49	1.39	1.89	57.52	0.70	82.2
	9.0	0.97	N/A	1.40	N/A	87.15	0.66	132.1
Hot water inside shower stall	5.1	5.1	7.25	1.54	1.31	2252	0.20	11260
	6.6	4.47	6.34	1.52	1.32	2395	0.32	7484
	9.0	5.2	7.49	1.57	1.35	2841	0.40	7103
Hot water outside shower stall	5.1	0.79	5.19	1.48	1.30	N/A	N/A	N/A
	6.6	1.0	5.22	1.51	1.23	N/A	N/A	N/A
	9.0	0.86	6.02	1.27	1.28	N/A	N/A	N/A

[a] Count median diameter.

[b] Mass median diameter.

[c] Geometric standard deviation.

[d] Generation rate.

[e] As defined in Eq. (2).

TABLE 3

Particle deposition fraction and dose for hot- and cold-water showering with mouth and nose breathing

	Flow rate (L/min)	TIWP[a] (mg)	Deposition fraction (%) mouth/nose					Deposition dose (mg) mouth/nose				
			ET[b]	BB[c]	bb[d]	Al[e]	Total	ET	BB	bb	Al	Total
Cold water	5.1	0.15	33.9/78.0	9.8/2.4	4.8/1.3	20.3/7.2	68.8/89.0	0.04/0.10	0.01/0.003	0.01/0.002	0.03/0.01	0.09/0.12
	6.6	0.29	28.4/70.9	8.0/2.2	4.1/1.3	19.7/8.3	60.7/82.7	0.07/0.18	0.02/0.01	0.01/0.003	0.05/0.02	0.15/0.21
	9.0	0.44	51.7/75.0	9.3/1.4	2.4/0.6	8.0/3.1	71.4/80.1	0.20/0.29	0.04/0.01	0.01/0.002	0.03/0.01	0.27/0.30
Hot water	5.1	11.26	60.3/87.1	15.6/1.8	4.4/0.5	7.2/1.0	87.5/90.3	6.59/9.51	1.70/0.19	0.48/0.06	0.78/0.11	9.56/9.87
	6.6	11.98	56.4/88.1	16.0/2.0	5.3/0.7	10.4/1.6	88.1/92.5	6.37/9.94	1.80/0.23	0.60/0.08	1.17/0.18	9.94/10.43
	9.0	14.21	60.7/86.3	15.0/1.7	4.1/0.5	6.8/0.9	86.7/89.4	8.52/12.11	2.11/0.24	0.58/0.07	0.95/0.13	12.16/12.55

[a] Total inhaled water particles.

[b] Extrathoracic region.

[c] Bronchial region.

[d] Bronchiolar region.

[e] Alveolar-interstitial region.

TABLE 4

Deposition dose for hazard materials

Flow rate (L/min^{-1})		Deposition dose for mouth/nose breathing (μg)					
		Cold water			Hot Water		
Material or Element	Concentration in water (ppm)	5.1	6.6	9.0	5.1	6.6	9.0
Total droplets	N/A	103/134	176/240	314/352	9852/10,168	10,554/11,082	12,320/12,704
Arsenic	0.035	$3.2/4.2 \times 10^{-6}$	$5.3/7.4 \times 10^{-6}$	$9.5/10.5 \times 10^{-6}$	$3.4/3.5 \times 10^{-4}$	$3.5/3.7 \times 10^{-4}$	$4.3/4.4 \times 10^{-4}$
Barium	0.2	$1.8/2.4 \times 10^{-5}$	$3.0/4.2 \times 10^{-5}$	$5.4/6.0 \times 10^{-5}$	$1.9/2.0 \times 10^{-3}$	$2.0/2.1 \times 10^{-3}$	$2.4/2.5 \times 10^{-3}$
Chromium	0.017	$1.5/2.0 \times 10^{-6}$	$2.6/3.6 \times 10^{-6}$	$4.6/5.1 \times 10^{-6}$	$1.6/1.7 \times 10^{-4}$	$1.7/1.8 \times 10^{-4}$	$2.1/2.1 \times 10^{-4}$
Fluoride	1.1	$9.9/13.2 \times 10^{-5}$	$1.7/2.3 \times 10^{-4}$	$3.0/3.3 \times 10^{-4}$	$1.1/1.1 \times 10^{-2}$	$1.1/1.2 \times 10^{-2}$	$1.3/1.4 \times 10^{-2}$
Nitrate	1.7	$1.5/2.0 \times 10^{-4}$	$2.6/3.6 \times 10^{-4}$	$4.6/5.1 \times 10^{-4}$	$1.6/1.7 \times 10^{-2}$	$1.7/1.8 \times 10^{-2}$	$2.1/2.1 \times 10^{-2}$
Trihalomethanes	0.008	$7.2/9.6 \times 10^{-7}$	$1.2/1.7 \times 10^{-6}$	$2.2/2.4 \times 10^{-6}$	$7.7/7.9 \times 10^{-5}$	$8.0/8.3 \times 10^{-5}$	$9.7/10 \times 10^{-4}$
Uranium	0.0071	$6.4/8.5 \times 10^{-7}$	$1.1/1.5 \times 10^{-6}$	$1.9/2.1 \times 10^{-6}$	$6.8/7.0 \times 10^{-5}$	$7.1/7.4 \times 10^{-5}$	$8.6/8.9 \times 10^{-5}$